

Spectroscopic and Differential Scanning Calorimetric Studies of the Order–Disorder Phase Transition in Bicyclononane

Ralph M. Paroli, Denis F. R. Gilson,¹ and Ian S. Butler

Department of Chemistry, McGill University, 801 Sherbrooke Street West, Montreal, Quebec H3A 2K6, Canada

Received June 6, 1997; in revised form September 15, 1997; accepted September 22, 1997

The phase transition in bicyclononane, C₉H₁₄O, has been examined using differential scanning calorimetry, variable-temperature vibrational spectroscopy, and proton spin–lattice relaxation time measurements. The high-temperature phase is disordered and the low-temperature phase either has an orthorhombic crystal with *D*₂ or *C*_{2v} symmetry or is tetragonal with *D*_{2d} symmetry. The barrier to rotation in the low-temperature phase between 250 and 300 K is 45.1 kJ mol⁻¹. In the high-temperature phase, two relaxation processes were observed, with activation energies of 11.7 (300–330 K) and 7.7 kJ mol⁻¹ (>330 K). © 1998 Academic Press

INTRODUCTION

Structures based on the bicyclo[3.3.1]nonane skeleton have received attention as a result of an unusually short intramolecular contact distance between hydrogens at C3 and C7, estimated to be less than 2.0 Å (1–4). In spite of this very close approach, the chair–chair conformations are of lowest energy but interconversion between the chair and boat forms is possible. The keto derivative, bicyclo[3.3.1]nonan-9-one, C₉H₁₄O, has interesting solid-state thermal properties. A recent adiabatic calorimetry study (5) reported a solid–solid phase transition at 300.5 K, with enthalpy and entropy changes of 14.11 kJ mol⁻¹ and 46.99 J K⁻¹ mol⁻¹, respectively. The entropy change is one of the largest observed for organic molecular crystals and indicates that considerable disorder must occur in the high-temperature phase (phase I). This confirmed the results of an NMR study, in which whole molecule motion was assumed to be responsible for the ¹³C spin–lattice relaxation (6) in the high-temperature phase. Although the chair–chair form of bicyclononane predominates in the vapor (7), interconversion between conformers in solution is fast on the time scale of ¹³C NMR measurements (8), and lanthanide-induced-shift measurements indicated that about 22% of the boat–chair conformation exists in solution at room

temperature (9). If conformational interconversions occur in phase I, this could provide an additional disordering mechanism and thus contribute to the large entropy change associated with the transition. No information on the crystal structures of the two phases of bicyclononane is available.

EXPERIMENTAL

Bicyclononane was obtained from Aldrich Chemical Co. and was sublimed immediately before use. Differential scanning calorimetric measurements were performed on a Perkin-Elmer DSC-7 calorimeter with temperature and enthalpy calibrations based on the phase and melting transitions of cyclohexane. The samples were scanned at 5 K min⁻¹ for both the cooling and heating directions. Proton spin–lattice relaxation times were measured by the inversion–recovery method, using a spin-lock CPS spectrometer operating at 33 MHz. Raman spectra were obtained using an Instruments S.A. spectrometer with a Jobin-Yvon U-1000 1.0-m double monochromator. The 514.5-nm line of an argon-ion laser was used for excitation with a laser power of 100 mW at the sample. The samples were contained in sealed glass capillary tubes mounted, using indium foil, on the cold finger of a Cryodyne Model 21 cryocooler. Infrared spectra were recorded on an Analect AQS-18 FT spectrometer. The samples were examined as KBr pellets, which were allowed to relax for 1 month before use.

RESULTS AND DISCUSSION

Only one solid–solid phase transition was observed by DSC, at 282 K on cooling and at 299 K on heating. No endotherms were observed on heating and so no glassy-crystalline state was produced. The transition enthalpy and entropy changes were 13.9 kJ mol⁻¹ and 46.5 J K⁻¹ mol⁻¹, respectively. These results are in excellent agreement with those obtained by White and Perrott using adiabatic calorimetry (5). In addition, the hysteresis in the transition temperature corresponds to the minimum observed at 285 K in the cooling rate in the adiabatic calorimetric study;

¹To whom correspondence should be addressed.

thus bicyclononane can exist in both orientationally ordered and orientationally disordered states at room temperature.

In the absence of X-ray diffraction data on the crystal structure, useful information can be obtained from the splitting of peaks in the vibrational spectra which depend upon the site and factor group symmetry in the crystal. A total of 66 Raman and 53 infrared bands are expected for the $C_9H_{14}O$ molecule with C_{2v} symmetry: $\Gamma = 20a_1 + 13a_2 + 17b_1 + 16b_2$. The a_1 , b_1 , and b_2 modes are both IR and Raman active, whereas the a_2 species are solely Raman active. Only 40 Raman and 36 IR bands were actually observed (Table 1). At ambient temperature both the Raman and infrared spectra contained broad vibrational peaks and the Raman spectrum of the lattice region showed

TABLE 1
Raman and Infrared Vibrational Frequencies (cm^{-1})
of Bicyclo[3.3.1]nonan-9-one

Phase I (300 K)		Phase II (150 K)		
Raman	IR	Raman	IR	
	2995 sh		2990 sh	}
2989 m	2990 vs	2984 m	2998 s	
	2965 sh			}
2958 w	2960 s		2960 sh	
2941 vs	2940 sh			}
2932 s	2932 vs			
		2926 vs		}
2917 vs	2916 vs		2920 vs	
2915 sh				}
2910 vs	2910 vs		2910 sh	
	2900 vs			}
2886 m				
2880 sh	2879 vs		2881 vs	}
2865 sh	2860 vs			
2855 s	2853 vs	2582 vs	2854 vs	}
	1733 w	1730 sh	1730 sh	
1719 w	1720 vs	1720 w	1722 vs	}
1709 w	1710 vs			
	1700 sh			}
1680 vw				
1490 vw		1490 vw	1496 vw	}
	1483 m			
1458 w	1457 m		1456 m	}
1455 w		1455 m		
	1447 m		1448 m	}
1440 vw				
1436 w	1435 vw	1438 m	1436 vw	}
1430 w				
	1408 vw			}
1365 sh	1368 w			
1363 vw	1358 vw		1358 w	}
		1356 vw		
1349 vw	1349 vw		1348 w	}
1335 vw				
	1328 m	1328 vw	1328 vw	}
	1316 m		1313 w	

TABLE 1—Continued

Phase I (300 K)		Phase II (150 K)		
Raman	IR	Raman	IR	
1292 m		1295 w		}
	1287 vw			
1280 vw				}
1271 vw	1275 vw			
	1254 vw		1257 w	}
1245 vw	1247 m		1244 w	
1240 s	1236 w	1235 sh	1240 sh	}
		1231 m		
		1228 sh		}
1218 vw	1220 m		1218 w	
		1186 sh		}
1165 w	1165 vw	1162 vw		
	1136 w			}
1125 w				
1123 w		1121 vw		}
1085 s	1088 vw	1081 s		
	1078 m	1075 m	1076 m	}
1068 m	1068 w		1070 w	
1029 w	1026 vw	1033 w	1025 vw	}
	1020 sh			
1004 w	1001 vw	1001 w	1001 vw	}
941 s	938 w	937 m	936 w	
929 vw	927 vw			}
920 vw	915 m		917 w	
907 vw	904 s	904 vw	904 m	}
834 w	830 sh	830 vw	830 sh	
	829 vw	828 vw	829 vw	}
807 s	804 vw	805 s	803 vw	
785 vw	784 vw		783 vw	}
754 w	753 w		752 w	
750 w	748 vw	750 w		}
735 vw	739 vw	729 w		
714 vw		714 vw		}
661 s	655 vw	661 m	655 vw	
		616 vw		}
605 vw	603 vw	605 vw	601 vw	
470 vw	474 w			}
	466 m		466 vw	
455 m	460 w	456 w		}
		430 vw		
		384 sh		}
		370 vw		
		340 vw		}
		305 vw		
		293 vw	288 vw	}
		228 vw	228 vw	
		221 vw		}
		120 m		
121 m				}
80 vw				
70 vw				}
55 vw				

only the broadened Rayleigh line and no discrete peaks. These observations are characteristic of an orientationally disordered solid. Upon cooling, the bands in the Raman spectrum became sharper and narrower and, by 150 K,

many peaks had split into two components and the lattice region now showed three peaks. Similarly, the IR bands narrowed or split into two peaks at low temperature (Figs. 1 and 2). Possible site symmetries are C_{2v} , C_2 , C_s , or C_1 , since the site symmetry must be equal to or lower than the molecular point group. The C_1 and C_i factor groups with a C_1 site would not lead to splitting of the vibrational peaks and the triclinic groups can be ruled out. Thus the most likely possibilities are (i) a D_2 crystal with a C_2 site or a C_{2v} crystal with a C_s site, (ii) a D_{2d} crystal with a C_s site, or (iii) S_4 or C_4 crystals with a C_1 site. For the first case, all Raman peaks and some infrared peaks should be doubled. In case ii all infrared peaks should be split into doublets and the Raman peaks split into two or into three peaks, and in case iii all Raman peaks split into three peaks. Since no splitting into three peaks was observed, the low-temperature phase is either orthorhombic, D_2 or C_{2v} , with two molecules per unit cell, or tetragonal, D_{2d} , with $Z = 4$.

Spin-lattice relaxation time measurements showed a sharp break in T_1 at the phase transition (Fig. 3) and also the hysteresis in the transition. In phase II, below 299 K, T_1 increased with decreasing temperature but at about 225 K, where values exceeded 20s, the signal-to-noise ratio deteriorated to the extent that the errors in T_1 were too great to give reliable values. It appeared, however, that T_1 may decrease again below 200 K. The plot of relaxation times versus reciprocal temperature gave an activation energy of 45.1 kJ mol^{-1} for the temperature region 250–300 K. In phase I there was a change of slope at about 330 K, with

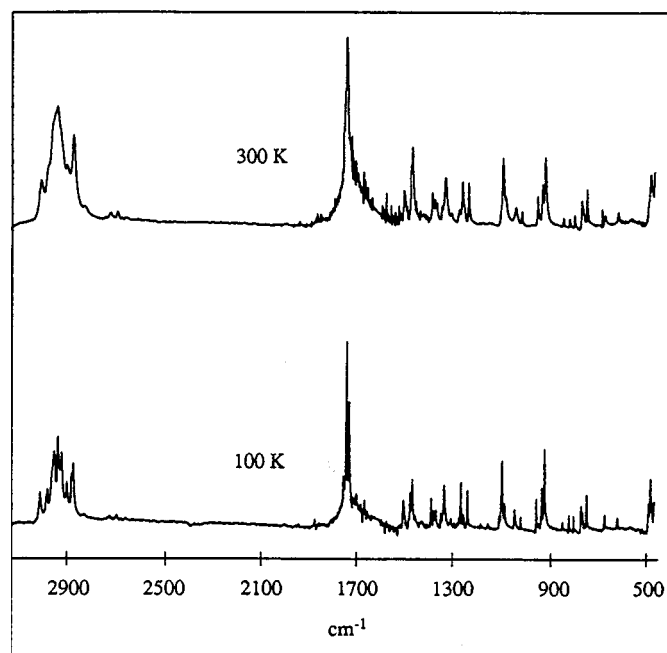


FIG. 1. Infrared spectra of bicyclononane: Phase I at 300 K; phase II at 100 K.

activation energies of 11.7 (between 300 and 330 K) and 7.7 kJ mol^{-1} (above 330 K), which are relatively low barriers. Since no T_1 minima were observed, no second-moment values could be obtained and it was not possible to determine which motions are responsible for relaxation.

Since the changes in molecular conformation are possibly involved in the disordering process, the energetics have been calculated by molecular mechanics methods. Similar calculations have been reported previously (3), but using a modified force field (2). The heat of formation calculated by the MM2 (10) method was $-249.9 \text{ kJ mol}^{-1}$ compared with $-232.6 \text{ kJ mol}^{-1}$ obtained by MM3 (11) and $-219.5 \text{ kJ mol}^{-1}$ from PCMODEL (Serena Software). The experimental value¹³ is $239.9 \text{ kJ mol}^{-1}$. Using the dihedral driver option in MM2, we calculated the energy as a function of the two dihedral angles, $C_1C_2C_3C_4$ and $C_1C_8C_7C_6$, on driving the structure from the chair-chair to the chair-boat and then to the boat-boat conformation. The latter structure is not symmetrical, as the rings adopt twist-boat conformations with dihedral angles of 36.7° and 58.5° . A contour plot of the MM2 energy is given in Fig. 4. The chair-boat form lies 4.8 kJ mol^{-1} above the chair-chair structure, with a barrier to interconversion of 22.7 kJ mol^{-1} . The boat-boat form is 18.5 kJ mol^{-1} above the chair-boat form, with a barrier of 15.9 kJ mol^{-1} . In the boat-boat form, there is a very small barrier of 4.0 kJ mol^{-1} between the two twisted structures; this value, however, is barely larger than the error in the calculation. Osawa and co-workers (3), using a harder torsional potential, obtained a difference of 10.9 kJ mol^{-1} and a barrier of 29.7 kJ mol^{-1} for the chair-chair to chair-boat forms. PCMODEL gave much smaller energy differences of 4.0 and 16.6 kJ mol^{-1} between the chair-chair, chair-boat, and boat-boat structures, respectively. The variations in calculated energies probably extend to the dihedral driver calculations of the barrier heights and are too large to permit assignment of the activation energies measured by spin-lattice relaxation to a given motion. In solution, the interconversion of conformers is fast on the NMR time scale (8), suggesting that the barrier is low. In phase I, isotropic rotation is the most probable cause of relaxation, plus, with increasing temperature, conformational motions of the cyclohexyl rings involving the chair-boat interconversions causing the additional relaxation. The maximum change in molecular dimensions is not large, as the distance between those hydrogen atoms which are the furthest apart increases from 5.31 to 5.85 \AA (from chair-chair to boat-boat). In the expanded disordered phase this should not be a problem and the interconversions of the rings might well be responsible for the additional spin-lattice relaxation in phase I, since, in this phase, intermolecular forces are not strong. In the calorimetric study (5), a significant contribution to the entropy of transition was attributed to the volume change, since the analogous compound 2-adamantanone (12), which

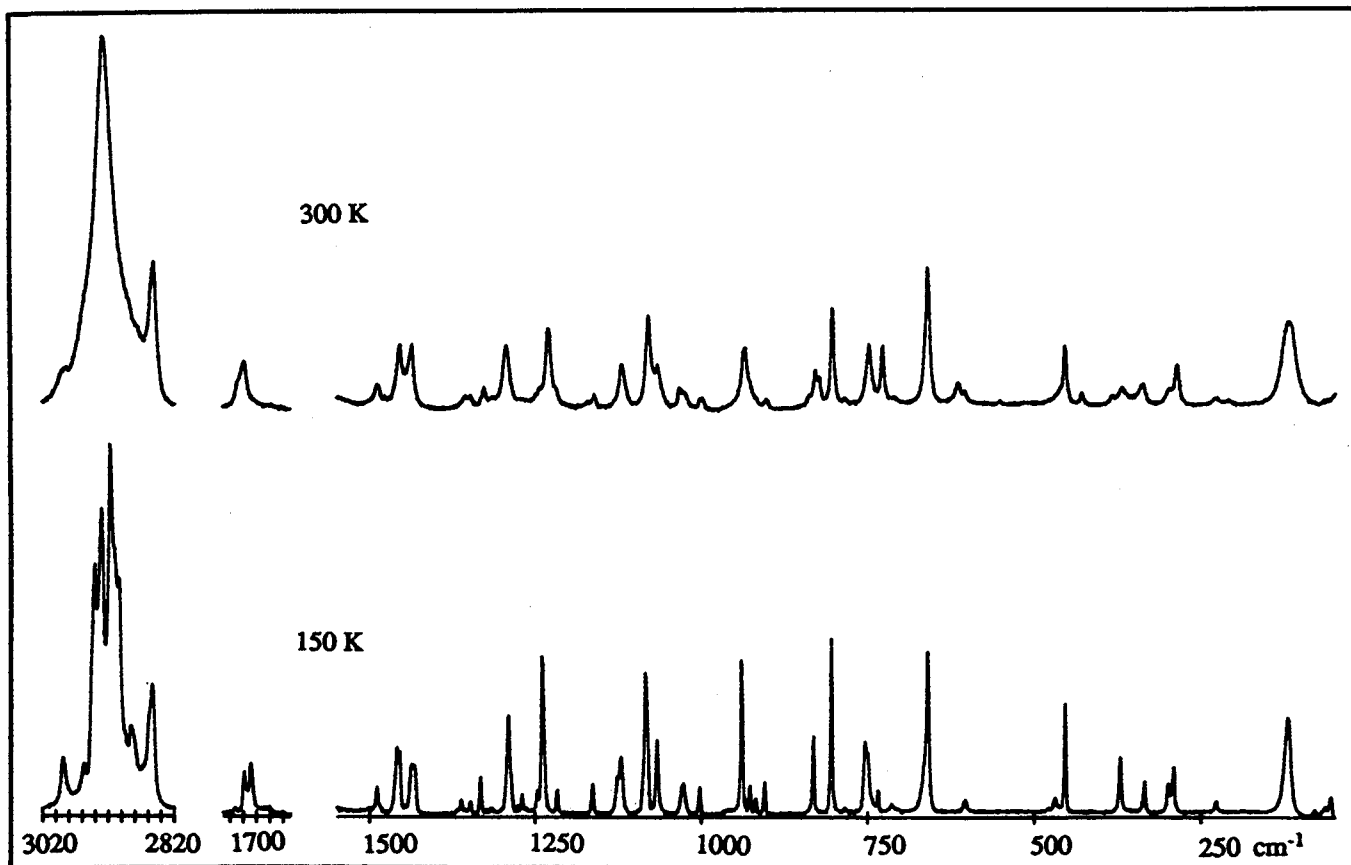


FIG. 2. Raman spectra of bicyclononane: Phase I at 300 K; phase II at 150 K.

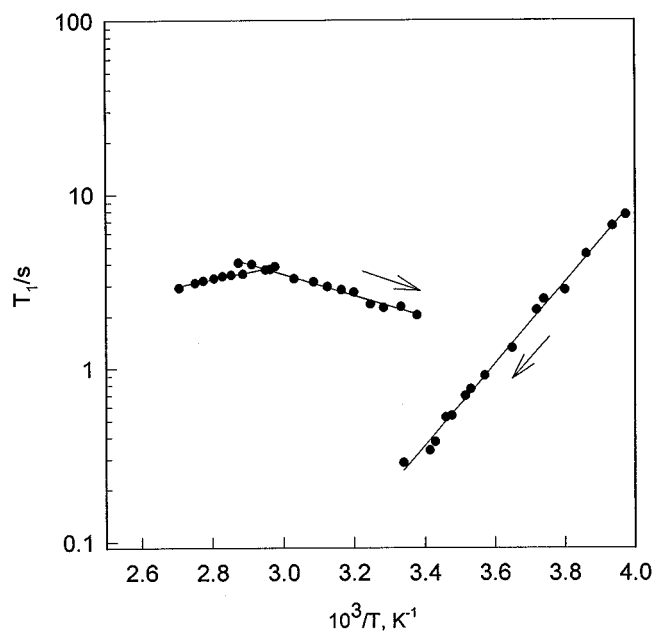


FIG. 3. Spin-lattice relaxation times versus reciprocal temperature.

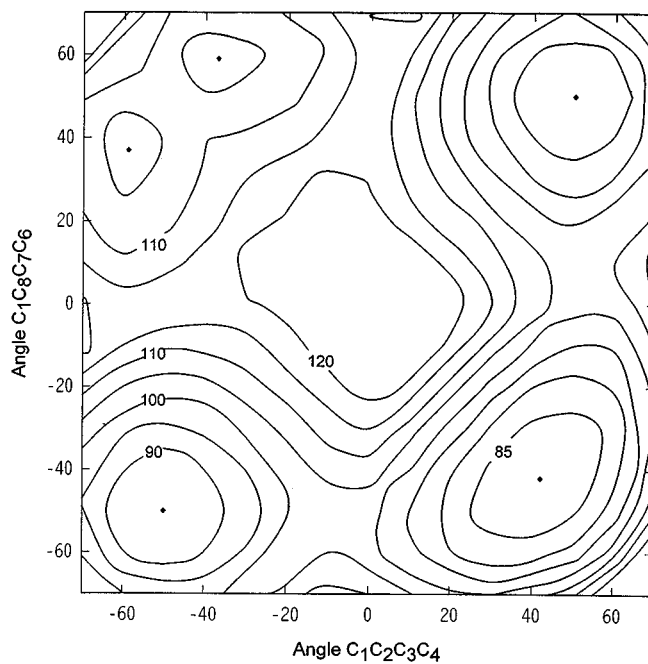


FIG. 4. Contour plot from dihedral driver calculations. Energies are in kJ mol^{-1} .

is rigid, had an entropy of transition that was much lower (the actual value depending on the thermal history of the sample). The upper limit of the temperature range covered by the adiabatic calorimetry study (5) was 306 K, and so any increased heat capacity from the conformational change was not observed, but this might contribute to the high value of the entropy of transition.

ACKNOWLEDGMENTS

This work was supported by grants from NSERC (Canada) and FCAR (Quebec).

REFERENCES

1. V. S. Mastryukov, M. V. Popik, O. V. Dorofeeva, A. V. Golubinski, L. V. Vilkov, N. A. Belokova, and N. L. Allinger, *J. Am. Chem. Soc.* **103**, 1333 (1981).
2. C. Jaime and E. Osawa, *Tetrahedron* **39**, 2769 (1983).
3. C. Jaime, E. Osawa, Y. Takeuchi, and P. Camps, *J. Org. Chem.* **48**, 4514 (1983).
4. N. L. Allinger, Y. H. Yuh, and J.-H. Lü, *J. Am. Chem. Soc.* **111**, 8551 (1989).
5. M. A. White and A. Perrot, *J. Solid State Chem.* **90**, 87 (1991).
6. R. E. Wasylishen and K. J. Friesen, *Org. Magn. Reson.* **13**, 343 (1980).
7. Y. S. Li and S. Li, *J. Mol. Struct.* **213**, 155 (1989).
8. D. L. Raber, C. M. Janks, M. D. Johnston, and N. K. Raber, *Tetrahedron Lett.* 677 (1980).
9. H.-J. Schneider, M. Lonsdorfer, and E. F. Weigand, *Org. Magn. Reson.* **8**, 363 (1976).
10. N. L. Allinger, *J. Am. Chem. Soc.* **99**, 8127 (1977).
11. N. L. Allinger, K. Chen, M. Rahman, and A. Pathiaseril, *J. Am. Chem. Soc.* **113**, 4505 (1991).
12. I. S. Butler, H. B. R. Cole, D. F. R. Gilson, P. D. Harvey, and J. McFarlane, *J. Chem. Soc., Faraday Trans. 2* **82**, 535 (1986).
13. J. D. Cox and G. Pilcher, "Thermochemistry of Organic and Organometallic Compounds." Academic Press, New York, 1970.